Conformationally Gated Rate Processes in Biological Macromolecules†

Yuri A. Berlin,‡ Alexander L. Burin,‡ Laurens D. A. Siebbeles,§ and Mark A. Ratner*,‡

Department of Chemistry, Center for Nanofabrication and Molecular Self-Assembly and Materials Research Center, Northwestern University, 2145 N Sheridan Road, Evanston, Illinois 60208-3113, and IRI, Radiation Chemistry Department, Delft University of Technology, Mekelweg 15, 2629 JB Delft, The Netherlands

Received: December 7, 2000; In Final Form: February 22, 2001

The concept of gating has been applied to the theoretical description of rate processes coupled to conformational rearrangements of biological macromolecules both out of equilibrium and near equilibrium. The out-of-equilibrium rearrangements are discussed in terms of requirements imposed by the complexity of biomolecules. These include (i) a variety of relaxation time scales for different degrees of freedom, (ii) constraints arising from their interactions, and (iii) the hierarchy of conformational substates. The simplest possible model that satisfies the requirements i−iii is developed. The model suggests that the motion along the reaction coordinate is gated by slower degrees of freedom. We show that under this assumption dynamics of the reaction coordinate resembles anomalous (non-Gaussian) diffusion. Expressions for observables derived within our model predict (i) a suppression of reaction coordinate dynamics in biomolecules imbedded in rigid matrixes, (ii) a transition from the familiar Debye exponential relaxation to the Kohlrausch−Williams−Watts relaxation described by a stretched exponential, and (iii) distinct temperature dependencies of relaxation rates for these relaxation processes. The experimental data on ligand binding to myoglobin support predictions i and ii. Coupling of rate processes to local conformational rearrangements near equilibrium has also been studied. As a particular example of such processes, we consider hole injection and transport in DNA molecular wires. Our treatment suggests that fluctuations in the mutual arrangement of base pairs in the stack can serves as a gate for both processes. This explains the unusual temperature dependence of the voltage gap found experimentally for poly(guanine)−poly(cytosine) molecular wires. The diffusion coefficient of holes and their mobility as a function of temperature are estimated for base pair stacks of varying structure.

1. Introduction

A common feature of biologically important molecules is a large number of conformational substates.[1] Due to transitions between the substates, the structure of the biological molecule imbedded in a solvent fluctuates and these fluctuations can drastically change the accessibility of reaction sites inside the molecule. Consequently, diffusion-controlled reactions of biological macromolecules, such as ligand binding to heme proteins, proceed with rates strongly affected by conformational fluctuations, and therefore, such reactions are characterized as rate processes coupled to the dynamics of reactant conformational rearrangements.

A convenient approach to model conformational dynamics is based on the concept of gating.[2] According to this idea, fluctuations serve as a gate that opens and closes the reaction binding site. The penetration of small ligands (O_2 and CO) into a heme "pocket" of myoglobin, when the motion of the protein chains permits the ligand to enter, furnishes a representative example of the gating mode, with the gate located on the protein. This particular example illustrates only one possible application of gating, which has also been used in several other biological contexts. These include the migration of small molecules through a protein matrix,[3] processes in biomembranes,[4] and biophysical aspects of medical therapies associated with reversible blocking of chemical reactions.[5]

Earlier theoretical works[2] treated gated reactions as diffusion-controlled processes affected by a certain stochastic (usually Markovian) impact. In the simplest two-state variant of theory,[2d,2h] the dynamics of the gate was assumed to be a stationary Markov process symbolized by the rate equation

$$\text{(open)} \underset{k_2}{\overset{k_1}{\rightleftharpoons}} \text{(closed)}$$

Theoretical analysis of this model situation allows the derivation of analytical expressions for the effective rate constant and the survival probability of reactants involved in gated reaction. Many-particle effects,[2h] the influence of reactant interactions on geminate and bulk diffusion-controlled processes,[2i] and the non-Boltzmann rate distributions in stochastically gated reactions[2j] were also studied. In all these cases, however, the concept of gating deals with a moving reactive particle as a whole and/or with large-scale changes in the geometry of reactants like, for instance, the opening of the "heme pocket". Another important aspect of the problem closely related to such fields of physical chemistry as "rate processes with dynamic disorder" [6] and "dispersive rate processes" [7] is gated coupling between various degrees of freedom of complex biomolecular objects.[8] The gated coupling implies that local rather than large-scale molecular rearrangements along a certain degree of freedom can be

† Part of the special issue "Edward W. Schlag Festschrift".

* Author e-mails. Y.A.B.: berlin@chem.nwu.edu. A.L.B: a-burin@chem.nwu.edu. L.D.A.S.: siebbeles@iri.tudelft.nl. M.A.R.: ratner@chem.nwu.edu.

‡ Northwestern University.

§ Delft University of Technology.

10.1021/jp004436c CCC: $20.00 © 2001 American Chemical Society
Published on Web 03/31/2001

considered as a gate for the local rearrangements along other degree of freedom. So far, this situation, which is known to be common for many biological macromolecules,[9] was studied insufficiently. This is especially true for the systems, where different degrees of freedom undergo relaxation over time scales organized hierarchically.

The present work is an attempt to fill the above gap in the description of rate processes in biological macromolecules. In particular, we explicitly treat the influence of hierarchic tiers on the dynamics of reaction coordinate. As a consequence, the detailed analysis of rate processes affected by conformational dynamics of biomolecules becomes possible. Two main types of conformational changes, i.e., local rearrangements at equilibrium and out of equilibrium, are discussed in detail. Both are able to affect a rate process proceeding in a biomolecular environment. As an example of nonequilibrium local rearrangements, in section 2, we consider conformational relaxation of certain degrees of freedom governing the rate of chemical reactions in proteins. A main interest is the situation commonly encountered in experimental studies of geminate ligand−heme recombination[9] and electron transfer in proteins,[10] where conformational changes are triggered by reactants inside the molecule due to excitation, for instance, by a short laser pulse. As a result, the reactant surroundings undergo relaxation from an initial nonequilibrium configuration toward the final equilibrium conformational state. For complex objects such as biomolecules, the relaxation process proceeds along many degrees of freedom and on many time scales. Since at least several of the coordinates specifying the relaxing degrees of freedom also define the height of the reaction barrier, the rate process is coupled to changes in the configuration of the complex molecular system, in which the chemical transformation occurs. The reaction dynamics can then be described in terms of nonequilibrium barrier crossing, frequently discussed in the literature[11] using a model similar to that proposed by Agmon and Hopfield.[12] This model as well as the Marcus−Sumi−Nadler investigation of dynamic solvent effects in electron-transfer processes[13] suggests that in addition to a reactant separation r arising due to bond breaking, there exists a gating coordinate x along which the reaction barrier should be overcome. To describe motion in the x-direction, we apply the concept of gating to the coupling between the reaction coordinate and other (usually slower) degrees of freedom. This suggests that relaxation of slower degrees of freedom responsible for large-scale conformational rearrangements opens the gate for the diffusive motion along the x-axis. As a consequence, the reaction coordinate can relax only if slower configuration changes "turn on" a green light for the migration along the coordinate x governing the rate of the barrier crossing and therefore the rate of reaction (the "traffic light" process). Using the simplest model possible, we demonstrate that the net effect of large-scale conformational rearrangements on the dynamics of reaction coordinate in proteins is anomalous (non-Gaussian) time-dependent diffusivity.[14] The latter arises only below a certain temperature prescribed by the energy distribution of protein conformational substates. Within the model proposed, the probability of reactants surviving in the course of the "traffic light" process and the time evolution of the reaction barrier are investigated. Our theoretical findings agree well with experimental observations for the standard test, geminate recombination of CO and heme iron in myoglobin.

A significant example of local conformation rearrangements studied in section 3 pertains to equilibrium fluctuations of torsional degrees of freedom, which control the efficiency of charge injection[15] and transport[16] over long distance in biological macromolecules. Being partially motivated by recent experiments on electrical conduction through individual DNA molecules,[17,18] we develop a theoretical model for hole injection and their transport controlled by fluctuation dynamics within the poly(guanine)−poly(cytosine) duplex. The model suggests that changes in the relative orientation or positions of two adjacent guanine bases slow the injection rate as the applied voltage approaches a threshold value. Like rate processes coupled to protein relaxation, the injection of charge carrier in DNA controlled by fluctuations in the mutual arrangement of nucleobases can also be treated as a "traffic light" process. In this case, however, "green" or "red" traffic lights for charge injection are turned on by fluctuations in the arrangement of guanine-cytosine (GC) base pairs inside the stack, since these affect the position of the HOMO level.[15,19] We demonstrate that for the poly(guanine)−poly(cytosine) duplex, our model yields nonlinear $I-U$ curves with a low-temperature voltage gap near 2.4 eV, in agreement with experimental observations.[18] Furthermore, these calculations suggest that for electric conductivity controlled by internal reorientation dynamics of stacked GC pairs the voltage gap becomes larger as temperature increases. This trend was indeed observed in experiments of Porath et al.,[18] but has remained unexplained. The conduction of DNA molecules as a function of temperature was also investigated above a voltage threshold where the band-like motion of charge carriers affected by torsions of base pairs can be described within the tight-binding approximation.[20] Numerical results show that the mobility of injected charges decreases with temperature and does not obey the familiar Arrhenius dependence. For systems where bridge-mediated charge transfer between donor and acceptor is controlled by changes in the relative orientation of mediators and where the equilibrium state is optimally overlapped, our theoretical treatment predicts a decrease of the tunneling transfer rate with temperature. This supports an earlier idea[21] concerning the effect of twisting motion on the conducting properties of polymers and on the variation of these properties with temperature.

2. Rate Processes Coupled to Conformational Relaxation

Let a biological macromolecule (e.g., a heme protein) with n degrees of freedom be subjected to slow conformational rearrangements triggered by the formation of reactive structures (for instance, an unbound ligand) and/or reaction sites (for example, an iron in the heme plane) inside the molecule at the time instant $t = 0$. Next, let us assume that for $t > 0$ a chemical reaction is coupled to the local rearrangements of the reaction site. The common approach used to take this coupling into account suggests that the specific reaction rate $k(x)$ depends on the conformational reaction coordinate x, while the population of conformational substates characterized by this coordinate evolves with time due to the diffusive motion in the x-direction.[11,12] This leads to the relaxation of the reaction coordinate considered as a local internal mode of the biomolecular object. Experiments[23−25] and general theoretical analysis of relaxation in strongly interacting systems[26] indicate, however, that this local mode should be coupled to the degrees of freedom distinct from x. Certain of them define more extended configurations of the object with much slower rate for attaining the equilibrium. The question now arises: To what extent are such global modes able to affect the dynamics of the conformational reaction coordinate and, hence, the rate of the reaction barrier crossing? The answer is of primary interest for clarifying such

issues as the protein role in the ligand-heme recombination[9] and in electron-transfer processes proceeding in the photosynthetic reaction center and other systems.[10a,b,i,j]

So far, the effect of global modes on the dynamics of the conformational reaction coordinate has been taken into account only implicitly by postulating that they may predetermine either parameters or the shape of the *x*-dependent part of the effective potential used to describe the ligation process.[11,12] By contrast, a class of models proposed here enables us to treat this effect explicitly. Models that fall into this class are based on the hierarchical structure of substates corresponding to local and global conformation rearrangements. Besides, they include constraints affecting the motion in the x-direction. In this regard, our theoretical description employs the same physical principles as those used for the formulation of the "spin-glass" models of relaxation.[26]

As an example, in the next section, we present the simplest hierarchic scheme with the constraint which allows the analytical treatment of the problem. This scheme is used in section 2.2 to the describe motion along the conformational reaction coordinate in the case where it can be affected by the relaxation of more global configurations of the biomolecular environment. The results obtained are used in section 2.3 to derive expressions for observables including the mean rate coefficient, the reaction barrier, and the survival probability. The calculated values of these quantities are compared with the experimental data reported for the geminate recombination of CO and heme iron in myoglobin.

2.1. Hierarchy and Constraint. Following the "spin-glass" models[26] and characteristic similarities of proteins and glasses,[27] we suppose that a successful theory of relaxation in biological macromolecules should satisfy three main requirements. First, the time behavior of the relaxing object should be described in terms of dynamics rather than in terms of statistics. This is particularly essential for biological macromolecules, which show certain common features with glasses. The latter systems are known to break ergodicity, so equilibrium distributions in configuration space are of little use. Second, the impossibility to diagonalize any reasonable nonlinear system into independent modes implies that the theory should involve constraints. They arise due to the interactions between various degrees of freedom and lead to the situation where, for example, atom X can move during or after relaxation of a spatially extended molecular unit Y. Third, a theoretical approach to the relaxation in complex systems should be based on a hierarchical scheme that takes proper account of dramatic distinctions between various degrees of freedom in the rates of attaining the equilibrium.[26,28,29]

A hierarchical scheme satisfying the requirements mentioned above can easily be constructed by realizing that the conformational reaction coordinate x serves as the demarcation line between quickly and slowly relaxing degrees of freedom.[29] Then the first tier of the hierarchy may be associated with j degrees of freedom equilibrated earlier than others. The most obvious example is the spatial separation r between a small ligand and the heme site of unligated protein.[12]

The second tier includes the local degree of freedom that controls the specific rate of the chemical process $k(x)$. For instance, in a particular case of ligand binding to heme proteins, x can be assigned to the distance between heme iron and the mean heme plane.[9,11,12]

The remaining motions are pooled to form the third tier of the hierarchy and are characterized by a set of coordinates y_i ($i \leq n - j - 1$). This tier involves degrees of freedom that determine conformation rearrangements of spatially extended structural units (for instance, due to the interaction of the unligated protein with the solvent) and governs the relaxation of the whole object or its essential parts toward the final equilibrium configuration. The latter process is modeled by sequential transitions of the system between conformational substates defined by random minima on the energy profiles presumably known for each y_i. Such global modes are assumed to constrain the rearrangements along the conformational coordinate usually approximated by diffusion in the harmonic potential.[11,12] The migration in the x-direction is allowed only in the course of conformational transitions along at least one of a number of coordinates y_i related to the third tier of the hierarchy; otherwise, changes in the position of the object on the x-axis are forbidden. Thus, the third tier is assumed to act as a gate for the motion along x-axis, so the time evolution of the conformational reaction coordinate becomes a "traffic light" process.

2.2. Motion along Conformational Reaction Coordinate. Taking into account the hierarchy of substates discussed in section 2.1, we turn now to a theoretical description of the constrained migration of the object in the x-direction. The following assumptions have been invoked to simplify the solution of the problem:

(i) The migration along the conformational reaction coordinate can be characterized by the diffusion coefficient D_x during each conformational transition in the third hierarchical tier, which removes the prohibition for the x-motion.

(ii) D_x increases with temperature T following the familiar Arrhenius law with the activation energy E_x and with the preexponential factor D_0.

(iii) On the third hierarchical tier, each event of conformational rearrangement involves three steps, namely, a thermal release from the local minima on the energy landscape, a fast motion toward the position of the next minimum, and a subsequent trapping there; these steps have typical time durations $\tau(E)$, τ_*, and τ_L, respectively, which satisfy the condition $\tau(E) \gg \tau_* \gg \tau_L$.

(iv) There are no correlations between positions of the object in the course of relaxation along various y_i.

(v) The number of relaxation pathways $q = n - j - 1$ on the third tier of the hierarchy is much greater than unity.

Of course, a fuller model might include a more branched hierarchy of time scales, correlations between different y_i, and the tunneling mechanism of transitions between conformational substates at each tier. However, we prefer the simplest model possible, since it suffices to gain understanding of the central physical phenomenon involved. Besides, current experimental detail does not justify the introduction of additional parameters and assumptions necessarily arising in extended variants of the theory.

The simple model formulated above offers the physical picture for the constrained dynamics of biological macromolecules schematically shown in Figure 1. According to this picture, each conformational transition along the ith relaxation pathway on the third tier allows a displacement in the x-direction with the probability

$$F_i = \frac{\tau_* + \tau_L}{\tau(E) + \tau_* + \tau_L} \approx \frac{\tau_*}{\tau(E)} \qquad (1)$$

where $\tau(E) = w_0^{-1} \exp[E/(k_B T)]$, w_0 is the frequency factor, and k_B is the Boltzmann constant. The approximate equality in

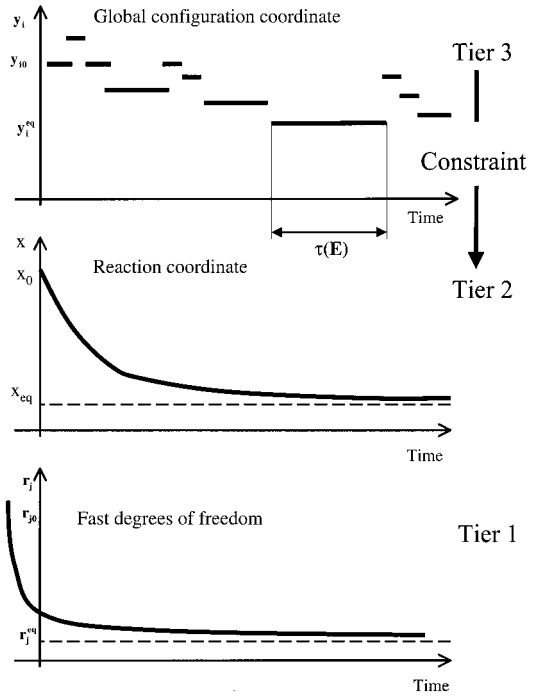

Figure 1. Simple hierarchy of conformational substates with gating constraint. Three hierarchical tiers involve degrees of freedom, specified by variables r_j, x, and y_i distinct in the rates of attaining their equilibrium values r_j^{eq}, x_{eq}, and y_j^{eq}. As seen from the lower panel, at $t = 0$, the relaxation at the first tier has already been completed, and the object is at a certain point of multidimensional conformational space with a set of coordinates $\{r_j^{eq},x_0,y_{i0}\}$. The random variables y_{i0} define the initially occupied local minima of energy profiles for each y_i and thus determine starting points for relaxation "trajectories" at the third tier. At $t > 0$, the object undergoes sequential transitions between the neighboring minima along any one of these trajectories. One of these global modes is presented in the upper panel, where solid horizontal lines correspond to the time $\tau(E)$ spent by a biological molecule in the minimum with the energy depth E. By virtue of the gating constraint, a green light for the motion in the x-direction flashes only during each of hopping events at the third tier. As a result, the global modes y_i govern the diffusive dynamics of local conformational changes at the second hierarchical tier, and the average of the conformational coordinate relaxes from the initial mean value $x = x_0$ toward its equilibrium value $x = x_{eq}$ (see middle panel).

the above expression for F_i corresponds to the assumption iii that enables one to neglect τ_L and $\tau_L + \tau_*$ in the numerator and in the denominator of eq 1. Since the relaxation along the conformational coordinates y_i is statistically independent (see assumption iv), the mean probability $\bar{F}(t)$ of the x-motion can be obtained by summing F_i over all i ($i = 0, 1, ..., q$) and averaging of the resultant ratio $q\tau_*/\tau(E)$ over the energy distribution, $P(E,t)$, of substates ("traps") occupied on the third hierarchical tier at time t. As a result, one gets

$$\bar{F}(t) = q\tau_* \int_0^\infty \frac{P(E,t)}{\tau(E)}\,dE = q\tau_* C(t) \qquad (2)$$

This implies that the population of conformational susbstates belonging to the second tier will propagate in the x-direction with the effective diffusion coefficient

$$D_{eff}(t) = D_x \bar{F}(t) = \Delta_0^2 \exp\left(-\frac{E_x}{k_B T}\right) C(t) \qquad (3)$$

where $\Delta_0 = (q\tau_* D_0)^{1/2}$.

The physical meaning of the obtained result is apparent. The product of first two factors in eq 3 represents the squared displacement in the x-direction during the period of time, when a "green" light for motion along the reaction conformational coordinate is "switched on" by the slow relaxation at the third hierarchical tier. Since $C(t)$ represents the mean frequency for the "green" light flashes, the effective diffusion coefficient $D_{eff}(t)$ is defined by the product of $C(t)$ and the squared displacement in the x-direction in accordance with eq 3.

To specify the integral $C(t)$ in eqs 2 and 3, it is instructive to note that the time evolution of distribution function $P(E,t)$ is described by the equation

$$\frac{dP(E,t)}{dt} = -\frac{P(E,t)}{\tau(E)} + \int_0^\infty W(E',E)\frac{P(E',t)}{\tau(E')}\,dE' \qquad (4)$$

Here $W(E',E)$ is the probability density that the object will undergo a transition from the substate with the energy between E' and $E' + dE'$ to the substate of the energy E. Since there are no preferential trapping sites for the temporal localization of the object due to the $E' \rightarrow E$ transition, $W(E',E)$ coincides with the distribution $g(E)$ pertaining to the third tier of the hierarchy. Hence, the solution of eq 4 can be written as

$$P(E,t) = g(E)\exp\left(-\frac{t}{\tau(E)}\right)\left[1 + \int_0^t C(t')\exp\left(\frac{t'}{\tau(E)}\right)dt'\right] \qquad (5)$$

Multiplying both sides of eq 5 by $\tau(E)^{-1}$ and performing the subsequent integration over all possible values of E, we arrive at the equation

$$C(t') = \int_0^\infty \frac{g(E)}{\tau(E)}\exp\left(-\frac{t}{\tau(E)}\right)dE + \int_0^t C(t')\int_0^\infty \frac{g(E)}{\tau(E)}\exp\left(-\frac{t-t'}{\tau(E)}\right)dE\,dt' \qquad (6)$$

This enables us to obtain $C(t)$ in the form of the Laplace transform. Indeed, putting

$$\Psi(s) = \int_0^\infty \frac{\tau(E)g(E)}{s\tau(E) + 1}\,dE \qquad (7)$$

one can verify that

$$C(s) = \int_0^\infty C(t)\exp(-st)\,dt = \frac{1}{s\Psi(s)} - 1 \qquad (8)$$

On the basis of physical arguments, $g(E)$ is usually assumed to decrease with E as the energy depth of conformational substates becomes equal to or higher than a certain value $E_* \geq 0$ (see, e. g., refs 11 and 12). In this case, the analysis allows us to specify the asymptotic temporal behavior of the effective diffusion coefficient in different temperature and time intervals. The results obtained are specified in Table 1. Note that in the high-temperature limit (i.e., at $T > T_{cr}$), $D_{eff}(t)$ turns out to be time independent, while in the low-temperature limit $T < T_{cr}$, there exists a rather wide time range, where this quantity evolves with t. Formally, the temporal behavior of D_{eff} is similar to the time evolution of the diffusion coefficient for anomalous (non-Gaussian) transport in one-dimensional systems with static energy disorder,[14] although physics of hierarchically constrained diffusion is distinct from physics of anomalous transport. The formal similarity can be expected, since the relaxation at the third hierarchical tier proceeds along large number of pathways with substates distinct in their energies and, therefore, the mean frequency of the "green" light flashes for the motion in the x-direction should decrease as the system visits deeper and deeper conformational substates. The similarity between anoma-

TABLE 1: Effective Diffusion Coefficient, $D_{\mathrm{eff}}(t)$, within Different Temperature and Time Intervals[a]

temp. ranges	time intervals: $t \ll \frac{1}{\langle 1/\tau(E)\rangle}$	$\frac{1}{\langle 1/\tau(E)\rangle} < t < \langle\tau(E)\rangle$	$t > \langle\tau(E)\rangle$
$T > T_{\mathrm{cr}} = \frac{\zeta(E_*)}{k_{\mathrm{B}}}$	$D_{\mathrm{eff}} = \Delta_0^{\,2} w_0 \exp\left(-\frac{E_x}{k_{\mathrm{B}}T}\right)$		
$T < T_{\mathrm{cr}} = \frac{\zeta(E_*)}{k_{\mathrm{B}}}$	$D_{\mathrm{eff}}(t) = D_{\mathrm{eff}} = \Delta_0^{\,2} \exp\left(-\frac{E_x}{k_{\mathrm{B}}T}\right)\left\langle\frac{1}{\tau(E)}\right\rangle$	$D_{\mathrm{eff}}(t) = \frac{\Delta_0^{\,2} \exp\left(-\frac{E_x}{k_{\mathrm{B}}T}\right)\sin(\pi T/T_{\max}(1/t))}{\pi k_{\mathrm{B}} T \Gamma(T/T_{\max}(1/t)) g(E_{\max}(1/t)) t}$	$D_{\mathrm{eff}}(t) = D_{\mathrm{eff}} = \Delta_0^{\,2} \exp\left(-\frac{E_x}{k_{\mathrm{B}}T}\right)\frac{1}{\langle\tau(E)\rangle}$

[a] Here $\zeta(E_*) = -1/\left.\frac{\mathrm{d}\ln g(E)}{\mathrm{d}E}\right|_{E=E_*}$, $E_{\max} = k_{\mathrm{B}}T\ln(w_0 t)$, $T_{\max} = \zeta(E_{\max})/k_{\mathrm{B}}$, and $\Gamma(z)$ is the gamma function. The brackets $\langle\cdots\rangle$ in expressions for $D_{\mathrm{eff}}(t)$ stand for the averaging over the energy distribution of conformational substrates belonging to the third hierarchical tier. Other notations are given in the text.

TABLE 2: Behavior of the Effective Diffusion Coefficient, $D_{\mathrm{eff}}(t)$, for the Exponential and Gaussian Energy Distributions of Conformational Substrates within Different Temperature and Time Intervals[a]

temp. ranges	time intervals: $t \ll \frac{1}{\langle 1/\tau(E)\rangle}$	$\frac{1}{\langle 1/\tau(E)\rangle} < t < \langle\tau(E)\rangle$	$t > \langle\tau(E)\rangle$
Exponential Energy Distribution $g(E) = \frac{1}{k_{\mathrm{B}}T_0}\exp\left(-\frac{E}{k_{\mathrm{B}}T_0}\right)$, $E > 0$			
$T > T_0$		$D_{\mathrm{eff}} = w_0\Delta_0^{\,2}\exp\left(-\frac{E_x}{k_{\mathrm{B}}T}\right)$	
$T < T_0$	$D_{\mathrm{eff}}(t) = D_{\mathrm{eff}} = \frac{w_0\Delta_0^{\,2}T}{T+T_0}\exp\left(-\frac{E_x}{k_{\mathrm{B}}T}\right)$	$D_{\mathrm{eff}}(t) = \Delta_0^{\,2}G_0\exp\left(-\frac{E_x}{k_{\mathrm{B}}T}\right)(w_0 t)^{\eta-1}$, $\eta = \frac{T}{T_0} < 1$, $G_0 = \frac{w_0\sin(\pi\eta)}{\pi\eta\Gamma(\eta)}$	
Gaussian Energy Distribution $g(E) = \frac{1}{(2\pi)^{1/2}k_{\mathrm{B}}T_0}\exp\left(-\frac{E^2}{2(k_{\mathrm{B}}T_0)^2}\right)$, $E > 0$			
$T > T_0$		$D_{\mathrm{eff}} = w_0\Delta_0^{\,2}\exp\left(-\frac{E_x}{k_{\mathrm{B}}T}\right)$	
$T < T_0$	$D_{\mathrm{eff}}(t) = D_{\mathrm{eff}} = \frac{w_0\Delta_0^{\,2}T}{T+T_0}\exp\left(-\frac{E_x}{k_{\mathrm{B}}T}\right)$	$D_{\mathrm{eff}}(t) = \Delta_0^{\,2}G_0\exp\left(-\frac{E_x}{k_{\mathrm{B}}T}\right)(w_0 t)^{\eta-1}$, $G_0 = \frac{w_0 T_0\sin(\pi\eta)}{(2\pi)^{1/2}T\Gamma(2\eta)}$, $\eta = \frac{T^2}{2T_0^{\,2}}\ln(w_0 t)$	$D_{\mathrm{eff}}(t) = D_{\mathrm{eff}} = w_0\Delta_0^{\,2}\exp\left(-\frac{T_0^{\,2}}{2T^2} - \frac{E_x}{k_{\mathrm{B}}T}\right)$

[a] Expressions are obtained from theoretical result summarized in Table 1.

lous transport and the "traffic light" process along the reaction conformational coordinate becomes particularly evident if $g(E)$ is taken in the form of exponential and Gaussian distributions. The comparison of our theoretical results for $D_{\mathrm{eff}}(t)$ (see Table 2) and those reported earlier for the diffusion coefficient in one-dimensional systems with static exponential and Gaussian energy disorder[14] shows that in these cases both the temperature and time dependences of two quantities becomes identical. Furthermore, similar to the diffusive motion in the one-dimensional energy landscape with static exponential and Gaussian disorder,[30] the temporal behavior of $D_{\mathrm{eff}}(t)$ in the low-temperature limit can be approximated within the time range $t < \langle\tau(E)\rangle$ by the function

$$D_{\mathrm{eff}}(t) = \frac{D_0}{(1+\omega t)^{1-\eta}} \tag{9}$$

where $D_0 = \Delta_0^{\,2}\langle\tau^{-1}(E)\rangle\exp[-E_x/(k_{\mathrm{B}}T)]$ and $\omega = w_0(\langle\tau^{-1}(E)\rangle/G_0)^{1/(1-\eta)}$, while parameters η and G_0 are specified in Table 2.

Once the explicit form of $D_{\mathrm{eff}}(t)$ is evaluated, the constrained dynamics of conformational changes at the second tier can be described in terms of the following differential equation for the population distribution $\rho_{x_0}^{\mathrm{dif}}(x,t)$

$$\frac{\partial\rho_{x_0}^{\mathrm{dif}}(x,t)}{\partial t} = D(t)\frac{\partial}{\partial x}\exp\left(-\frac{V(x)}{k_{\mathrm{B}}T}\right)\frac{\partial}{\partial x}\left[\exp\left(\frac{V(x)}{k_{\mathrm{B}}T}\right)\rho_{x_0}^{\mathrm{dif}}(x,t)\right] \tag{10}$$

Here the subscript x_0 in the notation of the distribution function implies that at $t = 0$ a biological macromolecule occupies conformational substate with $x = x_0$. To a first approximation, the potential $V(x)$ in eq 10 should be chosen as harmonic to be in conformity with the requirement that the position $x = 0$ corresponds to the local equilibrium configuration of the surroundings along the reaction coordinate. Besides, such a potential increases with x and hence makes the diffusive motion in the x-direction bounded. The latter circumstance fits the restriction evident physically, which forbids the biomolecular environment in local equilibrium to modify the configuration without limit.

To solve eq 10, we introduce a new variable

$$u(t) = \int_0^t D_{\mathrm{eff}}(z)\,\mathrm{d}z = \frac{D_0}{\eta\omega}[(1+\omega t)^{\eta} - 1] \qquad (11)$$

where the second equality sign corresponds to $D_{\mathrm{eff}}(t)$ given by eq 9. This enables us to reduce eq 10 to that used by Ornstein and Uhlenbeck[31] for description of Brownian motion in a harmonic potential with force constant f. For the initial condition

$$\rho_{x_0}^{\mathrm{dif}}(x,0) = \delta(x - x_0) \qquad (12)$$

the fundamental solution of eq 10 has a form of the Gaussian

$$\rho_{x_0}^{\mathrm{dif}}(x,u(t)) = (2\pi\sigma_{\mathrm{D}}^2)^{-1/2} \exp\left[-\frac{(x-\bar{x})^2}{2\sigma_{\mathrm{D}}^2}\right] \qquad (13)$$

with the mean x-value, $\bar{x}$, and the dispersion, σ_{D}^2, given by

$$\bar{x} = x_0 \exp[-fu(t)/(k_{\mathrm{B}}T)] \qquad (14)$$

$$\sigma_{\mathrm{D}}^2 = (k_{\mathrm{B}}T/f)[1 - (\bar{x}/x_0)^2] \qquad (15)$$

Equations 13−15 show that for the second hierarchical tier, the maximum of the population distribution $\rho_{x_0}^{\mathrm{dif}}(x,t)$ relaxes toward the local equilibrium position $x = 0$ as t increases. For short- and long-time limits, this process can be described in terms of the characteristic relaxation time τ_0. Substitution of eq 11 into eq 14 proves that for $t \ll 1/(\omega\eta)$

$$\tau_0 = \frac{k_{\mathrm{B}}T}{fD_0} \qquad (16)$$

whereas for $t > \omega^{-1}\exp(1/\eta)$

$$\tau_0 = \frac{1}{\omega}\left(\frac{\eta k_{\mathrm{B}}T\omega}{fD_0}\right)^{1/\eta} \qquad (17)$$

It should be mentioned that eqs 16 and 17 predict distinct temperature dependencies of the relaxation rate $W_{\mathrm{rel}} = 1/\tau_0$ for short and for long t. The prediction remains valid for $T < T_{\mathrm{cr}}$ and for any one of the familiar mechanisms of the allowed motion in the x-direction. In particular, if the motion is thermally activated, W_{rel} increases with T in the short-time limit $t \ll 1/\omega$, following the Arrhenius law. However, this law ceases to be true for long t, since the dispersion parameter η in eq 17 increases with T. As a consequence, in the long-time limit $t \gg 1/\omega$, the relaxation rate varies more sharply with temperature than one can expect reasoning from only the Arrhenius behavior of D_0.

These theoretical results provide a description of constrained conformational rearrangements that are able to influence the reactivity in large molecules under nonequilibrium conditions. The extent to which the reaction rate is affected by these rearrangements depends on the explicit form of the specific rate coefficient k as a function of x and manifests itself in variations of observables with time and temperature. In the next section, we evaluate the quantities of direct experimental interest combining the proposed model of constrained conformational changes with a model for the nonequilibrium barrier crossing frequently used in the literature.[11−13]

2.3. Calculations of Observables. The model considered in the previous section implies that the third tier of the hierarchy has no direct effect on the reactivity but modulates it by controlling the motion in the x-direction. Because of this, the reaction proceeds on the potential energy surface $U(r, x)$, which depends solely on variables r and x associated with the first and second tiers, respectively. Since for many surfaces of bimolecular collisions $U(r, x)$ allows local separability,[32] the specific rate coefficient $k(x)$ can be derived using methods discussed in ref 3a.

The explicit form of $k(x)$ needed for calculations of observables is particularly easy to obtain if the potential $U(r, x)$ for reaction products is the sum of two special terms.[3a,11] One term, $U(r)$, depends only on r and exponentially approaches the constant value δ_{s} as $r \to \infty$. Another is the harmonic x-dependent part $V(x) = fx^2/2$ with the force constant f. For this separable potential[3a,11,12]

$$k(x) = k_0 \exp[-\gamma(x_{\neq} - x)] \qquad (18)$$

where k_0 is the preexponential factor and $x_{\neq}$ is the value of the conformational coordinate corresponding to the most reactive substate. The parameter γ in eq 18 can be specified in terms of the shift, Δx, between equilibrium values of the conformational reaction coordinate for chemically active and chemically inactive states as

$$\gamma = f\Delta x/(3k_{\mathrm{B}}T) \qquad (19)$$

while $x_{\neq}$ is related to δ_{s} by the relation

$$x_{\neq} = \left(\delta_{\mathrm{s}} + \frac{1}{2}f(\Delta x)^2\right)/f(\Delta x) \qquad (20)$$

For $k(x)$ given by eq 18, the relaxation of the system from the initial substate $x = x_0$ toward substates with the lower reactivity can compete in rate with the chemical reaction proceeding at different configurations of the biomolecular environment. As a result, the mechanism of the entire process involves two parallel rate channels, which are responsible for the time evolution of the survival probability $S(x_0, t)$. The latter quantity can be evaluated invoking the method of prescribed diffusion,[3a,11c] which suggests that chemical reaction has a minor effect on the shape of the population distribution $\rho_{x_0}^{\mathrm{dif}}(x,t)$. Application to problem under consideration yields

$$S(x_0,t) = \exp(-\int_0^t \langle k(x_0,y)\rangle_x\,\mathrm{d}y) \qquad (21)$$

where $\langle k(x_0,u)\rangle_x$ is the time-dependent specific rate averaged over the solution of eq 10

$$\langle k(x_0,u)\rangle_x = \int_x k(h)\rho_{x_0}^{\mathrm{dif}}(h,t)\,\mathrm{d}h = k_0 \exp\left[-\gamma\left(x_{\neq} - \bar{x}(u) - \frac{1}{2}\gamma\sigma_{\mathrm{D}}^2(u)\right)\right] \qquad (22)$$

and $u = u(t)$ is given by eq 11 as before.

By virtue of eqs 18−20, the mean specific rate can be rewritten in the Arrhenius form $k = k_0 \exp[-H_{\mathrm{R}}/(k_{\mathrm{B}}T)]$, where H_{R} is the reaction barrier. The model, thus, predicts an increase of H_{R} with time due to the conformational relaxation of the reactant surroundings. Such an increase can be described in terms of the relaxation function

$$\Phi(t) = \frac{H_R(\infty) - H_R(t)}{H_R(\infty) - H_R(0)} = \exp\left(-\frac{f}{k_B T}u(t)\right)\frac{\left[1 - \frac{\Delta x}{6x_0}\exp\left(-\frac{f}{k_B T}u(t)\right)\right]}{1 - \frac{\Delta x}{6x_0}} \quad (23)$$

The above expression for $\Phi(t)$ can be simplified in two limiting cases. For $t \ll 1/\omega$, eq 23 gives

$$\Phi(t) = \exp(-t/\tau_0)\frac{\left[1 - \frac{\Delta x}{6x_0}\exp(-t/\tau_0)\right]}{1 - \frac{\Delta x}{6x_0}} \quad (24)$$

with the characteristic relaxation time τ_0 given by eq 16. However, in the long time domain where $t \gg 1/\omega$, instead of eq 24 one gets

$$\Phi(t) = \exp(-t^\eta/t_0^\eta)\frac{\left[1 - \frac{\Delta x}{6x_0}\exp(-t^\eta/t_0^\eta)\right]}{1 - \frac{\Delta x}{6x_0}} \quad (25)$$

where τ_0 is defined now according to eq 17. These two distinct time behaviors of the relaxation function imply that in the course of the conformational rearrangement of the reactant surroundings a transition exists from the Debye exponential relaxation to the Kohlrausch−Williams−Watts (KWW) relaxation[33] described by a stretched exponential.

2.4. Consequences for Experiments. The results presented above allow several experimental tests of the proposed theory. The most obvious candidate for comparison of theory and experiments is the recombination of carbon monoxide (CO) and the central heme iron of photolyzed carbonmonoxymyoglobin (MbCO), probed by different methods over wide ranges of time (1 ps to 1 ks), temperature (10−320 K), and solvent condition.[1,9,22−24] The low-temperature kinetics of this reaction shows that survival probability decreases with t following a nonexponential law. Such behavior is consistent with our model, which suggests that at low temperatures, the rate of transitions, $1/\tau_*$, between conformational substates belonging to the third hierarchical tier becomes small and the "red" traffic light forbids the motion in the x-direction, i.e., the displacement of the iron from the mean heme plane.[12] As a consequence, immediately after the laser flash, myoglobin (Mb) molecules become "frozen" in the variety of initial conformations x_0, which differ substantially in the barrier height, H_R, for CO rebinding and can be characterized by the inhomogeneous distribution $\rho(x_0)$. In this situation, the specific rate in eq 21 becomes time-independent, i.e., $\langle k(x_0,t)\rangle_x = k(x_0)$, and the mean survival probability can be calculated from the expression

$$\langle S(t)\rangle = \langle S(x_0,t)\rangle_{x_0} = \int_{x_0}\rho(x_0)\exp(-k(x_0)t)\,dx_0 \quad (26)$$

The above equation coincides with earlier theoretical results,[11,12] which provide[9] the adequate description of the low-temperature CO rebinding. A new prediction following from the present model is that the temporal behavior of the mean survival probability predicted by eq 26 can be observed also at high temperatures if MbCO is embedded in a rigid matrix able to suppress the conformational changes at the third hierarchical tier. Recent experimental studies of geminate CO rebinding in photolyzed MbCO in trehalose at room temperature[22] support this prediction. The results obtained allow the authors to conclude[22] that high solvent viscosity prevents both interconversion of conformational substates and relaxation in the interior of the protein, independent of temperature. This ceases to be true for a glycerol/water matrix with much smaller viscosity; then geminate rebinding slows down as T is increased through the solvent glass transition.[9] According to our model, the decrease of the reaction rate can be attributed to a conformational relaxation that leads to higher reaction barrier H_R, see eqs 23−25.

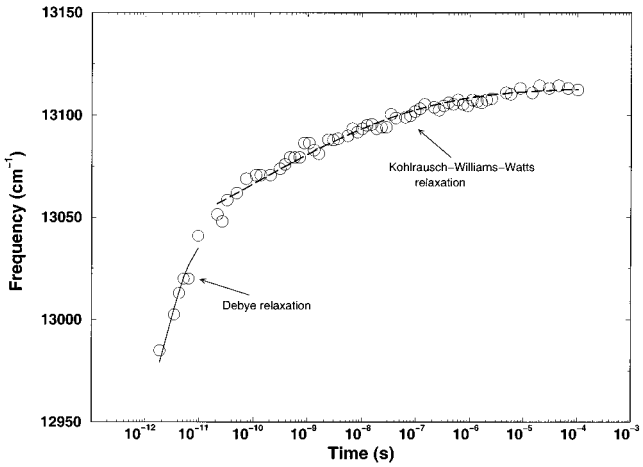

Figure 2. Temporal evolution of the center frequency $\bar{\nu}$ of band III after dissociation of CO−Fe bond in horse myoglobin. Open circles are experimental data.[23] Dashed and solid lines are obtained from eq 27 with the relaxation functions given by eq 24 and eq 25. For the exponential function (eq 24), $\tau_0 = 3.3$ ps; for the stretched exponential (eq 25), $\tau_0 = 0.7$ ps and $\eta = 0.1$. In both cases, $\Delta x/x_0 = 2.4$

Experimental information concerning the temporal behavior of the reaction barrier can be obtained by probing the time evolution of band III, a weak iron−porphyrin charge-transfer transition near 763 nm that is sensitive to the out-of plane position of the heme iron in Mb.[23] At $T = 301$ K, it has been found that $\bar{\nu}(t)$, the center frequency of the band, increases with t from $\bar{\nu}(0) = 12915$ cm^{-1} for the unrelaxed state with a nearly plane heme geometry to $\bar{\nu}(\infty) = 13113$ cm^{-1} assigned to the relaxed Mb with the equilibrium domed position of Fe atom. Since the displacement of the iron from the mean heme plane determines both the shift of the center frequency of band III and the barrier height for CO binding, these two processes should be described in terms of the same relaxation function $\Phi(t)$ defined by eq 23. Hence, based of the present model one can expect that

$$\bar{\nu}(t) = \bar{\nu}(0) + \Delta\nu(1 - \Phi(t)) \quad (27)$$

with $\Delta\nu = \bar{\nu}(\infty) - \bar{\nu}(0)$.

Comparison of eq 27 with the experimental dependence $\bar{\nu}$ versus t enables one to check whether the derived form of the Φ function can adequately reproduce relaxation kinetics. Data presented in Figure 2 show that eq 24 fits experimental results obtained at $t < 10$ ps, whereas eq 25 describes relaxation kinetics at longer times, over 7 decades. This allows the conclusion that the transition from the Debye exponential relaxation to the KWW nonexponential relaxation does occur in the course of conformational rearrangement of nonequilibrium protein structure. Note that according to our model, the relaxation process in the Debye and KWW regimes should exhibit different temperature dependence (cf. eq 16 and eq 17). For the Debye regime, the relaxation rate $W_{rel} = 1/\tau_0$ is expected to follow the

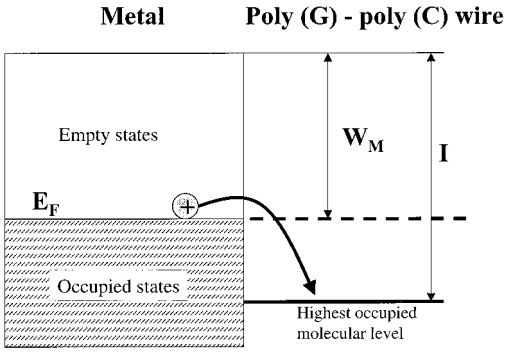

Figure 3. Energy levels for the metal−DNA contact. The metal work function W_M defines the position of the metal Fermi level E_F. A hole is injected to the highest occupied molecular orbital (HOMO) of the DNA whose ionization potential is I with respect to the vacuum level.

Arrhenius law. By contrast, the KWW relaxation is predicted to be non-Arrhenius. Experimental studies of the temperature effect on the time evolution of $\bar{\nu}$ are needed to check these theoretical predictions.

3. Rate Processes Coupled to Conformational Fluctuations

In this section, we consider processes in biological molecules near equilibrium, where they fluctuate between different conformations. Similar to relaxation events considered in section 2, these fluctuations are able to gate rate processes by what we call the "traffic light" mechanism. As has already been mentioned in Introduction, this situation is common for diffusion-controlled reactions.[2] Less is known about the effect of conformational fluctuations on the processes at the biomolecular/metal interfaces. Theoretical studies of such processes are important for gaining deeper understanding into physical mechanisms that might ensure the functioning of some structurally appropriate biomolecules as molecular wires.[15,16] Here we focus on this problem with a special emphasis on DNA, whose unique molecular structure makes this biomolecule particularly attractive for application in functional mesoscopic electronic devices[34] and in molecular computing.[35]

In the next section, we discuss main processes that determine the electrical conductivity of DNA molecules. A "traffic light" model for hole injection in a DNA wire is presented in section 3.2. As follows from numerical results considered in section 3.3, the same dynamic mode that "allows" a hole injection can affect the mobility of charge carriers generated on the wire. It is shown that both effects lead to an anomalous temperature dependence of the electrical conductivity, which decreases with T and does not follow the Arrhenius law.

3.1. Background. As in other molecular wires,[36,37] the electric current, I_{ec}, through the DNA molecule connecting two nanoelectrodes is determined by two processes, i.e., the injection of charge carriers onto the stack of base pairs and their transport along the stack. A central physical factor governing the efficiency of the injection is the location of the Fermi level, E_F, of the metallic contact relative to the energy levels of the stack. Obviously, the injection efficiency would be high if the Fermi level could align with one of the occupied or unoccupied molecular orbitals. However, it seems fairly certain that usually this is not the case. Instead, the Fermi level should fall in the HOMO−LUMO gap in order to preserve the charge neutrality of the "extended" molecule,[38] and the potential energy barrier will arise at the metal-molecular junction (Figure 3). In the absence of the electric field, the barrier height Δ_g that must be overcome to generate an "electronic" hole in the molecule with the ionization potential I can be approximated as [39]

$$\Delta_g = I - W_M \tag{28}$$

where W_M is the work function of the metallic contact.

The application of eq 28 for the estimation of Δ_g requires information about energetics of nucleobases within the stack. Experimental data on one-electron redox potentials of nucleobases in solution show that the energy of the hole when residing on adenine (A), cytosine (C), or thymine (T) bases is higher than that when on guanine (G) by 0.5−0.7 eV.[40] If the same trend is maintained in DNA, hole injection will proceed by electron transfer from the G site of the stack to metal. According to ab initio calculations,[19] the ionization potential of the G base is equal to 7.75 eV, and hence, eq 28 yields $\Delta_g = 2.39$ eV for DNA bridging two platinum contacts with work function 5.36 eV (see ref 41). Taking a typical barrier length as 5 Å,[42] it can be verified that thermally activated generation of holes is precluded, while the transmittance of their injection barrier for electron tunneling, $T(E_F)$, is about 4×10^{-3}. This implies that at low voltages (with much less than ∼1V being dropped across the molecule) the resistance R of the DNA wire evaluated from the Landauer formula $R = \hbar\pi/(e^2 T_{tun}(E_F)) = 12.9(k\Omega)/T_{tun}(E_F)$[43] is expected to be about 3.6 MΩ, in reasonable agreement the value measured by Fink and Schönenberger.[17] Thus, we conclude that at low bias the metal−molecular junction makes the main contribution to the conductance of the DNA wire.

The situation, however, becomes different at higher voltages, since the gap between the HOMO of G bases and the Fermi level of the contact decreases with increasing voltage U. In the vicinity of a certain voltage threshold, which corresponds to the energy crossing, the conduction of the DNA wire will be controlled by the ability of the base pair stack to transport a charge rather than by the efficiency of the injection process. Recent theoretical[44−49] and experimental[50−53] studies of long-range charge transfer in DNA show that a hole moves along stacks of AT and GC base pairs undergoing sequential tunneling transitions between neighboring G sites separated by fragments containing A and/or T bases. The basis of this hopping mechanism is that a guanine cation cannot oxidize A (or T or C) because of the larger ionization potential of A compared with that of G but can oxidize another G. According to standard electron transfer theory,[20,54] each oxidation step proceeds with the rate W_{hop}, which exponentially decreases with the length, L_{AT}, of the AT bridge between two adjacent G bases, i.e.

$$W_{hop} = W_0 \exp(-\beta L_{AT}) \tag{29}$$

where W_0 is the preexponential factor and β is the falloff parameter.

The direct consequence of eq 29 is the effect of arrangement and number of G bases in the stack on the hole mobility μ and therefore on the conductance of DNA wires near the voltage threshold. As follows from theoretical analysis[46,48] of charge-transfer experiments[50,51] performed for various base pair sequences, W_{hop} decreases by about a factor of 0.3 for each intervening AT base pair linked directly to the previous pair (like AA/TT) or about 1 order of magnitude for cross linked pairs (like AT/TA). Therefore, the highest mobility of holes along an AT−GC stack should be expected for base pair sequences with only one repeating AT pair between G bases. For these regular sequences, the value of the hole drift mobility can be evaluated from the Einstein relation

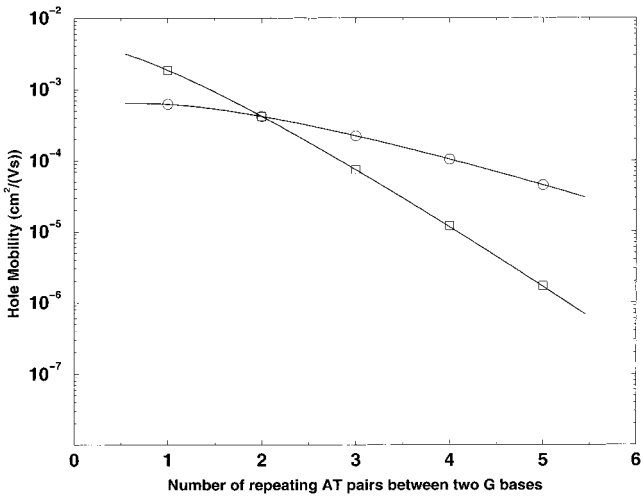

Figure 4. Hole mobility along a DNA wire composed of l repeating AT pairs between two adjacent G bases as a function of the number of AT base pairs within the bridge. The numerical results shown by circles and squares correspond to stacks with strands $G(TT)_lG(TT)_l$-$G(TT)_l$...$(TT)_lG$ and $G(TA)_lG(TA)_lG(TA)_l$...$(TA)_lG$, respectively.

$$\mu = \frac{e}{k_B T} D \cong \frac{e}{k_B T} W_{hop} L_{AT}{}^2 \tag{30}$$

where k_B is the Boltzmann constant, T is temperature, and D is the diffusion coefficient of holes. To determine the drift mobility from eq 30, we use the G−G hopping rate of about 10^9 s^{-1}, roughly estimated by Jortner et al.[45] for the strand GTTGTTGTT...TTG. For the sequence with one AT pair between G bases, this value should be larger by a factor of 3 due to the dependence of k_{hop} on the number of intervening AT pairs specified above. Taking the mean plane-to-plane distance between stacked bases to be equal to 3.4 Å,[55] we conclude that the hole mobility calculated from eq 30 for holes moving along the sequence with one repeating AT pairs between G bases is expected to be 2×10^{-3} cm^2 V^{-1} s^{-1} at room temperature. Similar estimates made for other regular sequences show that μ indeed decreases with the number of intervening AT pairs and depends on the particular base pairs stacked on the same strand (Figure 4).

Breaking of the positional order in the base pair sequences can dramatically reduce the mobility of holes undergoing hopping motion along the stack. There are two possible reasons for this effect. One reason lies in the fact that the hole mobility along the stack with irregular positions of G bases is determined by the time it takes for a charge carrier to jump through the longest AT fragments. Another reason is the existence of thermodynamic traps in sequences where several adjacent G bases are stacked on the same strand.[19,50] The origin of such traps can be understood within the tight-binding approach, which allows the calculation of the ionization potential of stacking G bases using the Hückel Hamiltonian

$$\hat{H} = \sum_{k=1}^{N} \epsilon_k n_k - b \sum_{k=1}^{N-1} (c_k^+ c_{k+1} + c_{k+1}^+ c_k)$$

$$n_k = c_k^+ c_k \tag{31}$$

Here c_n^+ and c_n are the creation and annihilation operators for a hole at nth site, respectively, b is the transfer integral, and ϵ_n is the energy of a hole at the nth site (for a single site ϵ_1 corresponds to the ionization potential I_1 of a single G base). The solution of the Schrödinger equation with the Hamiltonian

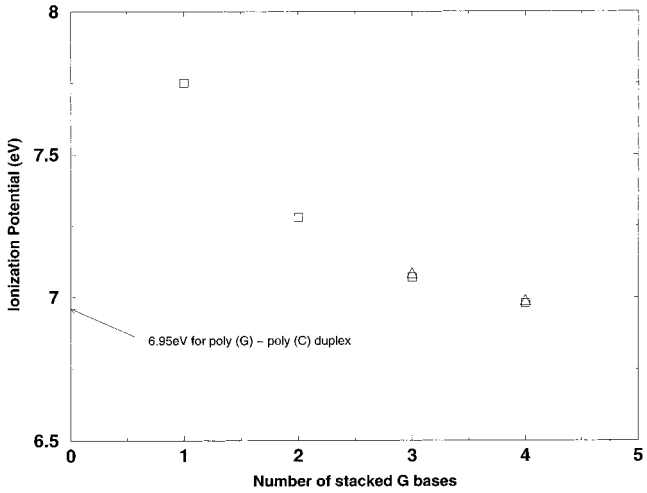

Figure 5. Dependence of the ionization potential on the number of G bases stacked on the same strand. The squares are ab initio calculations,[19] and the triangles are the results of tight-binding calculations; $b = 0.4$ eV, $I_1 = 7.75$ eV.

(31) enables one to estimate the ionization potential for any number, N_G, of stacked G in terms of the lowest energy needed to create one hole. The results of our tight-binding calculations with parameters $I_1 = 7.75$ eV and $b = 0.4$ eV are shown in Figure 5. As can be seen from the numerical results obtained, the ionization potential of the stacked G bases decreases with N_G in good agreement with the results of ab initio studies.[19] Accordingly, the energy of hole located, for instance, on GGG is lower than the energy of G^+ by about 0.7 eV, and hence, the triple GGG serves as a sink for moving hole in accord with experimental findings.[50]

It is interesting that in the limit of a large number of stacked G bases, the ionization potential moves toward the value $I_1 - 2b = 6.95$ eV that corresponds to the I value for the poly(G)−poly(C) duplex. The difference in ionization potentials for the individual G and for G bases stacked at the same strand can be explained by the formation of the band with width $2b$ due to $\pi-\pi$ interactions between neighboring GC pairs. Equation 28 then implies that for poly(G)−poly(C) oligomers, the energy barrier, Δ_g, for hole injection becomes smaller in comparison with irregular DNA stacks consisting of both AT and GC pairs. The lowering of the potential barrier, in turn, will reduce the voltage threshold, U_c, for poly(G)−poly(C) duplex as compared to that for irregular DNA.

To estimate U_c, we exploit the simplest model possible, which suggests that the potentials at the injecting and collecting contacts vary with the applied voltage as $W_M - U/2$ and $W_M + U/2$, respectively. If, in addition, one assumes that the applied field does not affect the electronic structure of stacked base pairs, the HOMO of the molecular wire will be expected to cross the Fermi level at the voltage

$$U_c = 2(I - W_M)/e = 2\Delta/e \tag{32}$$

Experimentally, the energy crossing manifests itself as the voltage gap in the observed $I_{ec}-U$ curves. Equation 32 is applicable to the evaluation of this observable only in the low-temperature limit, where the molecular motion in the stack is frozen and does not perturb the alignment of base pairs optimal for the injection process. Using the ionization potential of the poly(G)−poly(C) duplex calculated above, we conclude that in the case of platinum electrodes the voltage gap for the poly(G)−poly(C) molecular wire is about 3V. This crude estimate is

consistent with the experimental value reported by Porath et al.[18] for the poly(G)−poly(C) duplex between two platinum contacts at cryogenic temperatures.

3.2. Dynamic Model for Poly(G)−Poly(C) Duplex. To describe the injection of holes along the poly(G) strand at finite temperatures, the dynamics of the stack has to be taken into account, since different types of internal molecular motion observed in DNA on various time scales[56] can influence the coupling between the nearest-neighboring GC pairs in the poly(G)−poly(C) molecular wire. Particular dynamic modes that can affect the coupling include bending, flipping of bases,[57] and their twisting around the stack axis.[19] To avoid choice of the specific dynamic mode, which is currently not justified experimentally, it is convenient to introduce the conformational coordinate φ_i, which determines the relative arrangement of adjacent ith and (i+1)-th G bases. Then the potential energy associated with the conformational degree of freedom near the equilibrium position $\varphi_i = \varphi_{eq}$ can be approximated by

$$u_i = \frac{1}{2}F_s(\varphi_i - \varphi_{eq})^2 \tag{33}$$

with F_s being the stiffness constant.

The effect of molecular motion on the coupling within the stack is modeled by the dependence of the transfer integral, $b_{i,i+1}$, for sites i and $i+1$ on the coordinate φ_i. In analogy with eq 33, the explicit form of this dependence can be derived by expanding $b_{i,i+1}(\varphi_i)$ as power series in $(\varphi_i - \varphi_{eq})$. If we restrict ourselves to the terms of the second order in $(\varphi_i - \varphi_{eq})$, the result reads

$$b_{i,i+1}(\varphi_i) = b(1 - A(\varphi_i - \varphi_{eq}) - B(\varphi_i - \varphi_{eq})^2) \tag{34}$$

Such dependence on a conformational coordinate occurs very often, particularly for π-type chromophores.[21,58] Note that the coupling constants A and B in eq 34 depend on the position of the maximum for the transfer integral. If $b_{i,i+1}(\varphi_i)$ reaches the maximum value at $\varphi_i = \varphi_{eq}$ (i.e., at the equilibrium position of the conformational coordinate), then $A = 0$, and $B > 0$. This is particularly true for twisting motion in molecular conductors, as evident from earlier studies.[21,59] Once $b_{i,i+1}(\varphi_i)$ is specified, the derivation of the temperature dependence of the mean transfer integral $\langle b_{i,i+1}\rangle$ is straightforward. All we need to do is to average eq 34 over the Boltzmann distribution

$$w_B = \left(\frac{F_s}{2\pi k_B T}\right)^{1/2} \exp\left(-\frac{F_s(\varphi - \varphi_{eq})^2}{2k_B T}\right) \tag{35}$$

As a result, we get

$$\langle b_{i,j}\rangle = b(1 - B\langle(\varphi - \varphi_{eq})^2\rangle) \approx b\left(1 - B\frac{k_B T}{F_s}\right) \tag{36}$$

Thus, the transfer integral becomes smaller as temperature increases, since molecular rearrangements within the stack reduce $\pi-\pi$ interaction between adjacent G bases. Consequently, the ionization potential of the poly(G)−poly(C) duplex, which falls off with b, will increase, and the voltage gap U_c will widen with T linearly, as follows from eq 32 and eq 36. The slope and intercept of the linear dependence U_c versus T is given by

$$\frac{dU_c}{dT} \approx 4b\frac{k_B T}{eF_s} \tag{37}$$

$$U_c(0) = 2(I_1 - W_M - 2b)/e \tag{38}$$

Thus, we conclude that the voltage gap for the poly(G)−poly(C) wire does not obey the familiar Arrhenius law. Instead, the U_c values should linearly increase with T, following linear temperature dependence with the slope and the intercept given by eq 37 and eq 38, respectively. This trend was indeed observed for the poly(G)−poly(C) duplex.[18] Due to the wide scatter in the data, the obtained results provide only order-of-magnitude evaluation of the experimental slope which gives $dU_c/dT \approx 10^{-3}$ V/K.

3.3. Transport of Injected Holes Along a Poly(G)−Poly(C) Wire. In addition to the injection process considered in section 3.2, the conductivity of the poly(G)−poly(C) duplex will be determined by the drift mobility, μ, of generated holes along the molecular wire. The μ value can be estimated from the Einstein relation (see the first equality in eq 30), if the diffusion coefficient D for holes is known.

One simple estimate for the latter quantity is based on the time-dependent self-consistent field (TDSCF) approach[58] used earlier for studying charge motion in DNA.[44,49] This allows us to describe hole transport within the framework of the same dynamic model used in section 3.2 to treat the injection process. To investigate the effect of twisting motion on the diffusion of charge carriers, we modify the Hückel Hamiltonian (eq 31) by adding a term dependent on the angular coordinates $\varphi_i(t)$. As a result, the Hamiltonian for holes can be written as

$$\hat{H}_q = \sum_{k=1}^{N}\epsilon_k c_k^+ c_k - \sum_{k=1}^{N-1} b(\varphi_{k+1}(t) - \varphi_k(t))(c_k^+ c_{k+1} + c_{k+1}^+ c_k) \tag{39}$$

The twisting motion is described by the Hamiltonian

$$\hat{H}_{tw} = \frac{1}{2}\sum_{k=1}^{N}[\tilde{I}\,\dot{\varphi}_k^{\,2} + F_s(\varphi_{k+1}(t) - \varphi_k(t) - \varphi_{eq})^2] \tag{40}$$

where $\tilde{I}$ is the moment of inertia of a GC base pair.

The equation of motion along the conformation coordinate was obtained by averaging the Hamiltonian in eq 39 over the hole wave function $|\Psi(t)\rangle = \Sigma_k c_k(t)|k\rangle$ and adding the result to eq 40. Since initially a hole is assumed to be localized on the site with $k = 1$, the initial condition for the wave function is $c_1(t{=}0) = 1$ and $c_{k\neq 1}(t{=}0) = 0$.

The mean-square displacement of holes along the poly(G)−poly(C) wire defined as

$$\Delta_{wire}^2(t) = \sum_k |c_k(t)|^2 k^2 \tag{41}$$

was calculated exploiting the numerical procedure described earlier.[44,61b] In the calculations, the equilibrium angle, φ_{eq}, was taken to be equal to −36° on the basis of the data reported in refs 19 and 62. The moment of inertia, $\tilde{I}$, was calculated using the atomic coordinates of a GC base pair.[63] The values of F_s were the same as in section 3.2, and the angular-dependent charge-transfer integral $b(\varphi_{k+1}(t) - \varphi_k(t))$ was taken equal to half the energy difference of the HOMO−HOMO1 orbitals of stacked 5′-GG-3′, as calculated by Sugiyama and Saito.[19]

The calculated temperature and time dependencies of the mean-square displacement are plotted in Figure 6. As can be seen from the numerical data obtained, $\Delta_{wire}^2(t)$ linearly increases with t as long as the temperature remains constant. The slope of this linear dependence provides the diffusion coefficient of holes, since for one-dimensional motion $\Delta_{wire}^2(t) = 2Dt$.

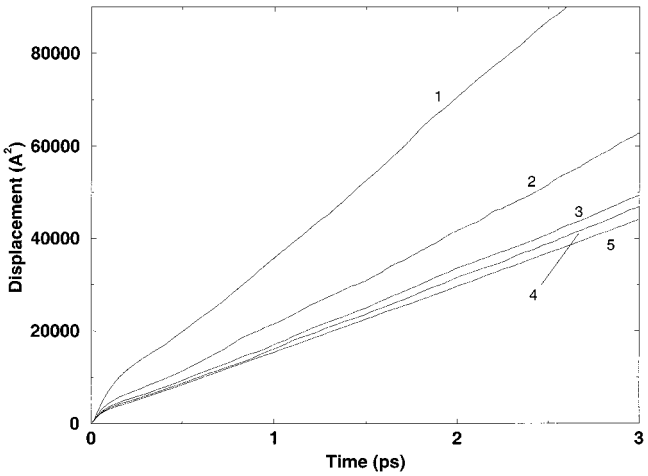

Figure 6. TDSCF time behavior of the mean-square displacement of holes in poly(guanine)−poly(cytosine) duplex at 293 K (curve 1), 200 K (curve 2), 150 K (curve 3), 100 K (curve 4), and 50 K (curve 5).

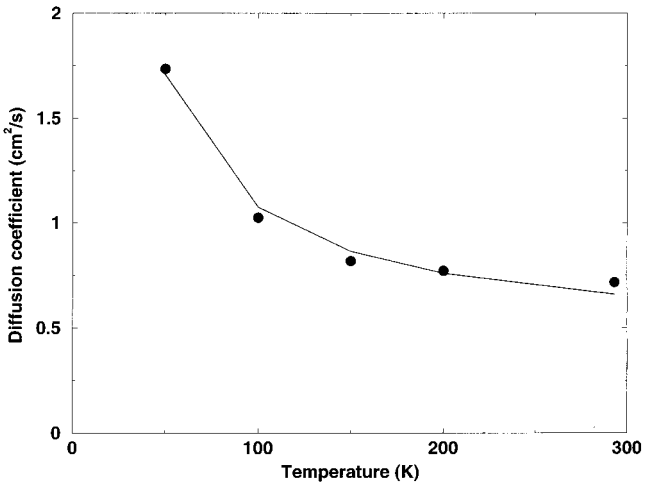

Figure 7. Temperature dependence of the diffusion coefficient for holes in poly(guanine)−poly(cytosine) duplex. Points are numerical results. Solid line is approximation according to eq 42.

Figure 7 shows that temperature reduces D, in contrast with the familiar Arrhenius law. This can be an additional reason for the anomalous temperature dependence of conductivity observed for poly(G)−poly(C) duplexes.[18] It is also evident that the numerical data on the temperature dependence of the hole diffusion coefficient can be approximated as

$$D(T) = D_1 + \frac{D_2}{T} \tag{42}$$

where D_1 and D_2 are constants equal to 0.44 cm^2/s and 63 cm^2 K s^{-1}, respectively. This functional form of the temperature dependence $D(T)$ is consistent with the scattering of moving holes by fluctuations of φ in the vicinity of its equilibrium value φ_{eq}.[64]

It should be noted that the temperature dependencies of the diffusion coefficient and the mobility of holes μ following from eqs 30 and 42 are distinct from those resulted from "conventional" electron−phonon interaction effects in condensed media. In the latter case, the mobility of quasi-free charge carriers varies with temperature as $T^{-3/2}$ (see ref 65). Due to the Einstein relation given by the first equality in eq 30, this implies that for holes in liquids and solids $D(t) \sim T^{-1/2}$. Thus, conformational fluctuations lead to stronger temperature dependencies of hole transport coefficients μ and D as compared with the "conventional" effects of electron−phonon interaction.

The numerical data on the diffusion coefficient suggest that the mobility of holes injected in the poly(G)−poly(C) duplex is high. If the value of the transfer integral used in our calculations is the upper limit of this parameter b, one can conclude that at room temperature μ should be less than or equal to 30 cm^2 V^{-1} s^{-1}. This value is much higher than the estimated values of the hole mobility in mixed stacks consisting of both AT and GC.

4. Conclusions

In summary, we have demonstrated that the concept of gating allows for deeper insight into the mechanism of rate process coupled to the conformational relaxation or conformational fluctuations in biological macromolecules. Applied to the equilibrium and nonequilibrium situations, this concept treats certain gated chemical reactions and transport phenomena in biologically important systems as "traffic light" rate processes. In the case of nonequilibrium biomolecular environment, we proposed the class of models which describe the effect of global dynamic modes of the biological object on the time evolution of the local conformational coordinate x governing the specific rate $k(x)$ of the barrier crossing. The general results obtained in section 2.2 show that in the vicinity of a certain temperature T_0, prescribed by the energy distribution of conformational substates, the global modes give rise to the smooth transition from the normal Gaussian diffusion in the x-direction to the anomalous non-Gaussian dynamics. The latter process is characterized by the time-dependent diffusion coefficient $D(t)$ moving toward distinct asymptotic values in the short- and long-time limits. These theoretical findings justify the dispersion model for small ligand binding to heme proteins, which suggests that diffusion along the conformational reaction coordinate should be considered as the non-Gaussian process in view of characteristic similarities of proteins and glasses.

The expressions for observables derived within the framework of our model predict that the coupling of local and global modes can manifest itself experimentally as (i) the suppression of the reaction coordinate dynamics in biomolecules imbedded in rigid matrix and (ii) a transition from the familiar Debye exponential relaxation to the KWW relaxation described by a stretched exponential. The experimental data on the reaction barrier available for ligand binding to myoglobin strongly support this prediction. In addition, we showed that Debye and KWW relaxation processes could be distinguished by their temperature dependencies: the former process follows the familiar Arrhenius law, while the latter is found to be non-Arrhenius.

As an example of "traffic light" rate processes at the biomolecular/metal interfaces which are affected by fluctuations, we have considered hole injection and transport in stacks of Watson−Crick base pairs in B-form DNA. Our analysis focused on two types of stacks, which differ in the arrangement and number of guanine bases involved. The stacks of the first type consist of irregular sequences of pyrimidine and purine deoxynucleotides, while the second involves regular stacks containing only guanine−cytosine pairs. It has been shown that despite this structural distinction, the general feature of the injection process turns out to be common for both types of molecular wire: in both cases, the motion of charge carriers in the metal−DNA junction proceeds via tunneling controlled by internal fluctuation dynamics of the stack. A theoretical model developed for this mechanism of hole injection in the poly(guanine)−poly(cytosine) duplex predicts linear increase of the voltage gap with

temperature and provides estimates for the slope and the intercept, which are in reasonable agreement with available experimental data. We also used a simple dynamic TDSCF model for studying transport of holes along regular stacks containing only guanine−cytosine pairs. As follows from the numerical results obtained, the diffusion coefficient and the mobility of holes decrease with temperature due to the scattering by fluctuations of the twisting angle between adjacent base pairs. This, together with the linear increase of the voltage gap with temperature, explains the anomalous temperature dependence of conductivity found for poly(guanine)−poly(cytosine) molecular wires. The upper limit of the hole drift mobility estimated from our numerical results show that charge carrier transport proceeds more effectively in poly(guanine)−poly(cytosine) duplex than along irregular stacks of pyrimidine and purine deoxynucleotides. This conclusion is consistent with results of recent experiments on charge transfer in DNA.

Acknowledgment. This research is supported by funding from the DoD/MURI program and the Chemistry divisions of NSF and ONR. We are grateful to M. E. Michel-Beyerle and to J. Jortner for helpful remarks. This is dedicated to Ed Schlag, teacher, scholar, and friend.

References and Notes

(1) Frauenfelder H.; Petsko, G. A.; Tsernoglu, D. *Nature* **1979**, *280*, 558. Parak, F.; Knapp, E. W.; Kuchieda, D. *J. Mol. Biol.* **1982**, *161*, 177. Goldanskii V. I.; Krupyanskii, Yu. F.; Flerov, V. N. *Sov. Biophys. Dokl.* **1983**, *272*, 209. Doster, W.; Cusack, S.; Petry, W. *Nature* **1989**, *337*, 754. Nienhaus, G. U.; Young, R. D. *Encyclopedia Appl. Phys.* **1996**, *15*, 163. Rejto, P. A.; Freer, S. T. *Prog. Biophys. Mol. Biol.* **1996**, *66*, 167.

(2) (a) McCammon, J. A.; Northrup, S. H. *Nature* **1981**, *293*, 316. (b) Northrup, S. H.; Zarrin, F.; McCammon, J. A. *J. Phys. Chem.* **1982**, *86*, 2314. (c) McCammon, J. A.; Harvey, S. C. *Dynamics of Protein and Nucleic Acids*; Cambridge University Press: Cambridge, 1987. (d) Szabo A.; Shoup, D.; Northrup, S. H.; McCammon, J. A. *J. Chem. Phys.* **1982**, *77*, 4484. (e) Hoffman, B. M.; Ratner, M. A.; Wallin, S. A. *Adv. Chem. Ser.* **1990**, *226*, 126. (f) Kim, J.; Lee, S. *Bull. Korean Chem. Soc.* **1992**, *13*, 398. (g) Spouge, J. L. *J. Phys. Chem. B* **1997**, *101*, 5026. (h) Makhnovskii, Yu. A.; Berezhkovskii, A. M.; Sheu, S.-Y.; Yang, D.-Y.; Kuo, K.; Lin, S. H. *J. Chem. Phys.* **1998**, *108*, 971. (i) Shushin, A. I. *J. Chem. Phys. A* **1999**, *103*, 1704. (j) Baker, N. A.; McCammon, J. A. *J. Phys. Chem. B* **1999**, *103*, 615.

(3) (a) Agmon N.; Rabinovich, S. *J. Chem. Phys*. **1992**, *97*, 7270; Wang, J.; Wolynes, P. *Chem. Phys.* **1994**, *180*, 141. (b) Eisenberg, N.; Klafter, J. *J. Chem. Phys.* **1996**, *104*, 6796;

(4) Cáceres, M. O.; Budde, C. E.; Ré, M. A. *Phys. Rev. E* **1995**, *52*, 3462. Budde, C. E.; Cáceres, M. O.; Ré, M. A. *Europhys. Lett.* **1995**, *32*, 205.

(5) Spouge, J. L.; Szabo, A.; Weiss, G. H. *Phys. Rev. E* **1996**, *54*, 2248.

(6) Buhks, E.: Jortner, J. *J. Chem. Phys*. **1985**, *83*, 4456. Zwanzig, R. *Acc. Chem. Res.* **1990**, *23*, 148. Granek, R.; Nitzan, A. *J. Chem. Phys.* **1990**, *92*, 1329; **1990**, *93*, 5918. Lonergan, M. C.; Nitzan, A.; Ratner, M. A. *J. Mol. Liq.* **1994**, *60*, 269.

(7) Plonka, A. *Prog. Reac. Kinet. Mech.* **2000**, *25*, 109.

(8) Berlin, Yu. A. *Chem. Phys.* **1996**, *212*, 29. Berlin, Yu. A.; Burin, A. L. *Chem. Phys. Lett.* **1997**, *267*, 234.

(9) Steinbach, P. J.; Ansari, A.; Berendzen, J.; Braunstein, D.; Chi, K.; Cowen, B. R.; Ehrenstein, D.; Frauenfelder, H.; Johnson, J. B.; Lamb, D. C.; Luck, S.; Moutant, J. R.; Neinhaus, G. U.; Osmos, P.; Philipp, R.; Xie, A.; Young, R. D. *Biochemistry* **1991**, *30*, 3988. Frauenfelder, H.; Wolynes, P. *Phys. Today* **1994**, *47*, 58. Schlichting, I.; Berendzen, J.; Phillips, G. N.; Sweet, R. M. *Nature* **1994**, *371*, 808. Parak, F.; Prusakov, V. E. *Hyperfine Interactions* **1994**, *91*, 885. Nienhaus, G.; Mourant, J. R.; Chu, K.; Frauenfelder, H. *Biochemistry* **1994**, *33*, 13413. Johnson, J. B.; Lamb, D. C.; Frauenfelder, H.; Muller, J. D.; McMahon, B.; Nienhaus, G. U.; Young, R. D. *Biophys. J.* **1996**, *71*, 1563. Sage, J. T.; Champion, P. M. In *Comprehensive Supramolecular Chemistry*; Suslick, K. S., Ed.; Pergamon: New York, 1996; Vol. 5, Chapter 6, p 171. Scott, E. E.; Gibson, Q. H. *Biochemistry* **1997**, *36*, 11909. Sugimoto, T.; Unno, M.; Shiro, Y.; Dou, Y.; Ikeda-Saito, M. *Biophys. J* **1998**, *75*, 2188. Esquerra, R. M.; Goldbeck, R. A.; Kim-Shapiro, D. B.; Kliger, D. S. *Biochemistry* **1998**, *37*, 17527. Brunori, M.; Cutruzzola, F.; Savino, C.; Travaglini-Allocatelli, C.; Vallone, B.; Gibson, Q. H. *Biophys. J.* **1999**, *76*, 1259. Ostermann A.; Waschipky, R.; Parak, F. G.; Neinhaus, G. U. *Nature* **2000**, *404*, 205.

(10) (a) Kleinfeld, D.; Okamura, M. Y.; Feher, G. *Biochemistry* **1984**, *23*, 5780. (b) Brunschwig, B. S.; Sutin, N. *J. Am. Chem. Soc.* **1989**, *111*, 7454. (c) Heitele, H. *Angew. Chem., Int. Ed. Engl.* **1993**, *32*, 359. (d) Cartling, B. *Biophys. Chem.* **1993**, *47*, 123. (e) Hoffman, B. M.; Ratner, M. A. *Inorg. Chim. Acta* **1996**, *243*, 233. (f) Trinkunas, G.; Holzwarth, A. R. *J. Phys. Chem B* **1997**, *101*, 7271. (g) McMahon, B. H.; Muller, J. D.; Wraight, C. A.; Nienhaus, G. U. *Biophys. J* **1998**, *74*, 2567. (h) Ogrodnik, A.; Hartwich, G.; Lossau, H.; Michel-Beyerle, M. E. *Chem. Phys.* **1999**, *244*, 461. (i) Olesen, K.; Ejdeback, M.; Crnogorac, M. M.; Kostic, N. M.; Hansson, O. *Biochemistry* **1999**, *38*, 16695. (j) Pletneva, E. V.; Fulton, D. B.; Kohzuma, T.; Kostic, N. M. *J. Am. Chem. Soc.* **2000**, *122*, 1034. (k) Bell, T. D. M.; Jolliffe, K. A.; Ghiggino, K. P.; Oliver, A. M.; Shephard, M. J.; Langford, S. J.; Paddon-Row M. N. *J. Am. Chem. Soc.* **2000**, *122*, 10661.

(11) (a) Berlin, Yu. A.; Chekunaev, N. I.; Goldanskii, V. I. *Chem. Phys. Lett.* **1992**, *197*, 81. (b) Gudowska-Novak, E. *J. Phys. Chem.* **1994**, *98*, 5257. (c) Berlin, Yu. A.; Fischer, S. F.; Chekunaev, N. I.; Goldanskii, V. I. *Chem. Phys.* **1995**, *200*, 369. (d) Agmon, N.; Sastry, G. M. *Chem. Phys.* **1996**, *212*, 207. (e) Pechukas, P. *J. Chem. Phys.* **1997**, *107*, 2444. (f) Agmon, N.; Krissinel, E. B. *Chem. Phys. Lett.* **1998**, *294*, 79.

(12) Agmon, N.; Hopfield, J. J. *J. Chem. Phys.* **1983**, *79*, 2042.

(13) Sumi, H.; Marcus, R. A. *J. Chem. Phys.* **1986**, *84*, 4894; Nadler, W.; Marcus, R. A. *Isr. J. Chem.* **1990**, *30*, 69. Sumi H. *Adv. Chem. Phys.* **1999**, *107*, 601.

(14) Scher, H.; Montroll, E. M. *Phys. Rev. B* **1977**, *12*, 2455. Alexander, S.; Berlasconi, J. Orbach, R.; Schneider, W. R. *Rev. Mod. Phys.* **1981**, *53*, 175. Bässler, H. *Phys. Status Solidi B* **1981**, *107*, 9. Chekunaev, N. I.; Berlin, Yu. A.; Flerov, V. N. *J. Phys. C* **1983**, *15*, 1219. Haus, J.; Kehr, K. W. *Phys. Rep.* **1987**, *150*, 265. Bässler, H. In *Hopping and Related Phenomena*; Fritzche, H., Pollak, M., Eds.; World Scientific: Singapore, 1989; p 491. Bouchaud, J. P.; Georges, A. *Phys. Rep.* **1990**, *195*, 127. Scher, H.; Schlesinger, M. F.; Bendler, J. T. *Phys. Today* **1991**, *44*, 26. Berlin, Yu. A.; Burin, A. L. *Chem. Phys. Lett.* **1996**, *257*, 665. Siebbeles, L. D. A.; Berlin, Yu. A. *Chem. Phys. Lett.* **1997**, *265*, 460.

(15) Berlin, Yu. A.; Burin, A. L.; Ratner, M. A. *Superlattices Microstruct.* **2000**, *28*, 241.

(16) Weinkauf, R.; Aicher, P.; Wesley, G.; Grotemeyer, J.; Schlag, E. W. *J. Phys. Chem.* **1994**, *98*, 8381. Weinkauf, R.; Schanen, P.; Yang, D.; Soukara, S.; Schlag, E. W. *J. Phys. Chem.* **1995**, *99*, 11255. Weinkauf, R.; Schanen, P.; Metsala, A.; Schlag, E. W.; Birgle, M.; Kesler, H. *J. Phys. Chem.* **1996**, *100*, 18567. Schlag, E. W.; Lin, S. H.; Weinkauf, R.; Rentzepis, P. M. *Proc. Natl. Acad. Sci. U.S.A.* **1998**, *95*, 1358. Baranov, L. Ya.; Schlag, E. W. *Z. Naturforsch.* **1999**, *54a*, 387. Schlag, E. W.; Sheu, S.-Y.; Yang, D.-Y.; Selzle, H. L.; Lin, S. H. *J. Phys. Chem. B* **2000**, *104*, 7790. Schlag, E. W.; Sheu, S.-Y.; Yang, D.-Y.; Selzle, H. L.; Lin, S. H. *Proc. Natl. Acad. Sci. U.S.A.* **2000**, *97*, 1068.

(17) Fink, H.-W.; Schönenberger, C. *Nature* **1999**, *398*, 407.

(18) Porath, D.; Bezryadin, A.; de Vries, S.; Dekker, C. *Nature* **2000**, *403*, 635.

(19) Sugiyama H.; Saito, I. *J. Am. Chem. Soc.* **1996**, *118*, 7063.

(20) Schatz, G. C.; Ratner, M. A. *Quantum Mechanics in Chemistry*; Prentice Hall: Englewood Cliffs, NJ, 1993.

(21) Pietro, W. J.; Marks, T. J.; Ratner, M. A. *J. Am. Chem. Soc.* **1985**, *107*, 5387. Hale P. D.; Ratner M. A. *J Chem. Phys.* **1985**, *83*, 5277.

(22) Hagen, S. J.; Hofrichter, J.; Eaton, W. A. *Science* **1995**, *269*, 959. Hagen, S. J.; Hofrichter, J.; Eaton, W. A. *J. Phys. Chem.* **1996**, *100*, 12008.

(23) Jackson, T. A.; Lim, M.; Anfinrud, P. A. *Chem. Phys.* **1994**, *180*, 131.

(24) Cordone, L.; Galajda, P.; Vitrano, E.; Gassmann, A.; Ostermann, A.; Parak, F. *Eur. Biophys. J* **1998**, *27*, 173.

(25) Lichtenegger, H.; Doster, W.; Kleinert, T.; Birk, A.; Sepiol, B.; Vogl, G. *Biophys. J.* **1999**, *76*, 414.

(26) Palmer, R. G.; Stein, D. L.; Abrahams, E.; Anderson, P. W. *Phys. Rev. Lett.* **1984**, *53*, 958.

(27) Iben, I. E. T.; Braunstein, D.; Doster, W.; Frauenfelder, H.; Hong, M. K.; Johnson, J. B.; Luck, S.; Osmos, P.; Schulte, A.; Steinbach, P. J.; Xie, A. H.; Young, R. D. *Phys. Rev. Lett.* **1989**, *62*, 1918. Frauenfelder, H.; Sligar, S. G.; Wolynes, P. G. *Science* **1991**, *254*, 1598. Frauenfelder H.; Wolynes P. G.; Austin, R. H. *Rev. Mod. Phys.* **1999**, *71*, S419.

(28) Shlesinger, M. F.; Klafter, J. In *Fractals in Physics*; Pietronero L., Tosatti, E., Eds.; Elsevier: Amsterdam, 1986; p 393. Blumen, A.; Klafter, J.; Zumofen, G. In *Fractals in Physics*; Pietronero L., Tosatti, E., Eds.; Elsevier: Amsterdam, 1986; p 399.

(29) Berlin, Yu. A. *Chem. Phys.* **1996**, *212*, 29. Berlin, Yu. A.; Burin, A. L. *Chem. Phys. Lett.* **1997**, *267*, 234.

(30) Berlin, Yu. A.; Siebbeles, L. D. A.; Zharikov A. A. *Chem. Phys. Lett.* **1997**, *276*, 361.

(31) Wang, M. C.; Uhlenbeck, G. *Rev. Mod. Phys.* **1975**, *17*, 323 and references therein.

(32) Levine, R. D.; Bernstein, R. B. *Molecular Reaction Dynamics and Chemical Reactivity*; Oxford University Press: New York, 1987.

(33) Kohlrausch, R. *Ann. Phys. (Leipzig)* **1847**, *12*, 393. Williams, G.; Watts, D. C. *Trans. Faraday. Soc.* **1970**, *66*, 80.

(34) Mirkin, C. A.; Letsinger, R. L.; Mucic, R. C.; Stofhoff, J. J. *Nature* **1996**, *382*, 607. Alivisatos, A. P.; Johnson, K. P.; Wilson, T. E.; Loveth, C. J.; Bruchez, M. P.; Schultz, P. G. *Nature* **1996**, *382*, 609. Okata, Y.; Kobayashi, T.; Tanaka, K.; Shimomura, M. *J. Am. Chem. Soc.* **1998**, *120*, 6165. Braun, E.; Eichen, Y.; Sivan, U.; Ben-Joseph, G. *Nature* **1998**, *391*, 775. Winfree, E.; Liu, F.; Wenzler, L. A.; Seeman, N. C. *Nature* **1998**, *394*, 539. Storhoff, J. J.; Mirkin, C. A. *Chem. Rev.* **1999**, *99*, 1849. Mao, C. D.; Sun, W. Q.; Shen, Z. Y.; Seeman, N. C. *Nature* **1999**, *397*, 144.

(35) Adleman, L. M. *Science* **1994**, *266*, 1021. Faulhammer, D.; Cukras, A. R.; Lipton, R. J.; Landweber, L. F. *Proc. Natl. Acad. Sci. U.S.A.* **2000**, *97*, 1385.

(36) For general discussion, see: Datta, S. *Electronic Transport in Mesoscopic Systems*; Cambridge University Press: Cambridge, 1995. Imry, Y. *Introduction to Mesoscopic Physics*; Oxford University Press: New York, 1997.

(37) For review, see: Ratner, M. A.; Davis, B.; Kemp, M.; Mujica, V.; Roitberg, A.; Yaliraki, S. *Ann. New York Acad. Sci.* **1998**, *852*, 22. Mujica, V.; Nitzan, A.; Mao, Y.; Davis, W.; Kemp, M.; Roitberg, A.; Ratner, M. A. *Adv. Chem. Phys.* **1999**, **107**, 403.

(38) Xue, Y.; Datta, S.; Ratner, M. A. Submitted to *Phys. Rev. Lett*.

(39) Pope, M.; Swenberg, C. E. *Electronic Processes in Organic Crystals*; Oxford University Press: New York, 2000.

(40) Seidel, C. A. M.; Schultz, A.; Sauer, M. H. M. *J. Phys. Chem.* **1996**, *100*, 5541. Steenken S.; Jovanovic, S. C. *J. Am. Chem. Soc*. **1997**, *119*, 617. There is the uncertainty concerning the difference in energies of holes located on G and three other nucleobases. However, the exact value of this difference is not crucial for the phenomenological model proposed. The key point for our further theoretical analysis of ground-state hole migration in DNA is that the gap between the lower oxidation potential of G and higher oxidation potentials of other nucleobases should be much larger than the thermal energy at room temperature. This is consistent with observations of selective oxidation of G bases in DNA (for review, see: Borrow, C. J.; Muller, J. G. *Chem. Rev.* **1998**, *98*, 1109−1151. Armitage, B. *Chem. Rev.* **1998**, *98*, 1171−1200. Schuster G. B. *Acc. Chem. Res.* **2000**, *33*, 253−260.).

(41) *Handbook of Chemistry and Physics*, 47th ed.; The Chemical Rubber Co.: Cleveland, 1966; pp E−68.

(42) Samanta, M. P.; Tian, W.; Datta, S.; Henderson, J. I.; Kubiak, C. P. *Phys. Rev. B* **1996**, *53*, R7626.

(43) Landauer, R. *IBM J. Res. Dev.* **1957**, *1*, 223. Hereafter, e and $\hbar$ will denote electronic charge and Planck's constant, respectively.

(44) Grozema, F. C.; Berlin, Yu. A.; Siebbeles, L. D. A. *Int. J. Quantum Chem.* **1999**, *75*, 1009.

(45) Bixon, M.; Giese, B.; Wessely, S.; Langenbacher, T.; Michel-Beyerle, M. E.; Jortner, J. *Proc. Natl. Acad. Sci. U.S.A.* **1999**, *96*, 11713.

(46) Berlin, Yu. A.; Burin, A. L.; Ratner M. A. *J. Phys. Chem. A* **2000**, *104*, 443.

(47) Bixon, M.; Jortner, J. *J. Chem. Phys. B* **2000**, *104*, 3906.

(48) Berlin, Yu. A.; Burin, A. L.; Ratner, M. A. *J. Am. Chem. Soc.* **2001**, *123*, 260.

(49) Grozema, F. C.; Berlin, Yu. A.; Siebbeles, L. D. A. *J. Am. Chem. Soc*. **2000**, *122*, 10903.

(50) Meggers, E.; Michel-Beyerle, M. E.; Giese, B. *J. Am. Chem. Soc.* **1998**, *120*, 12950.

(51) Giese, B.; Wessely, S.; Spormann, M.; Lindemann, U.; Meggers, E.; Michel-Beyerle, M. E. *Angew. Chem., Int. Ed. Engl.* **1999**, *38*, 996.

(52) Henderson, P. T.; Jones, D.; Hampikian, G.; Kan, Y.; Schuster, G. B. *Proc. Natl. Acad. Sci. U.S.A.* **1999**, *96*, 8353.

(53) Lewis, F. D.; Wu, T. F.; Liu, X. Y.; Letsinger, R. L.; Greenfield, S. R.; Miller, S. E.; Wasielewski, M. R. *J. Am. Chem. Soc.* **2000**, *122*, 2889. Lewis, F. D.; Liu, X.; Liu, J.; Miller, S. E.; Hayes, R. T.; Wasielewski, M. R. *Nature* **2000**, *406*, 51.

(54) For general discussion, see: Ratner, M. A.; Jortner, J. *Molecular Electronics*; Blackwell: Oxford, 1997. Bixon, M.; Jortner J. *Adv. Chem. Phys.* **1999**, *106*, 35−208. Kuznetsov, A. M.; Ulstrup, J. *Electron Transfer in Chemistry and Biology*; Wiley: Chichester, 1999.

(55) Fukui, K.; Tanaka, K. *Angew. Chem., Int. Ed. Engl.* **1998**, *37*, 158. Kelley, S. O.; Barton, J. K. *Chem. Biol.* **1998**, *5*, 413.

(56) See, e.g.: Wennmalm, S.; Edman, L.; Rigler, R. *Chem. Phys.* **1999**, *247*, 61. Schuerman G. S.; Van Meervelt, L. *J. Am. Chem. Soc.* **2000**, *122*, 232. Liang, A.; Freed, J. H.; Keyes, R. S.; Bobst, A. M. *J. Phys. Chem.* **2000**, *104*, 5372 and references therein.

(57) Núñez, M. N.; Hall, D. B.; Barton, J. K. *Chem. Biol.* **1998**, *6*, 85.

(58) Toutounji, M. M.; Ratner, M. A. *J. Phys. Chem A* **2000**, *104*, 8566.

(59) Gutfreund, H.; Hartstein, C.; Weger M. *Solid State Commun.* **1980**, *36*, 647. Conwell, E. M. *Phys. Rev. B* **1980**, *22*, 1761.

(60) Lister, D. S.; Macdonald, J. N.; Owen N. L. *Internal Rotation and Inversion*; Academic Press: London, 1978.

(61) (a) Gerber, R. B.; Ratner, M. A. *Adv. Chem. Phys.* **1988**, *70*, 97. (b) Siebbeles, L. D. A.; Berlin, Yu. A. *Chem. Phys.* **1998**, *238*, 97.

(62) Conwell, E. M.; Rakhmanova, S. V. *Proc. Natl. Acad. Sci. USA* **2000**, *97*, 4556.

(63) Taken from: *Nucleic Acid Database*; The State University of New Jersey: Rutgers, NJ (http://ndbserver.rutgers.edu). See also: Rozenberg, H.; Rabinovich, D.; Frolow, F.; Hegde, R. S.; Shakked, Z. *Proc. Natl. Acad. Sci.* **1998**, *95*, 15194.

(64) Berlin, Yu. A.; Burin, A. L.; Siebbeles, L. D. A.; Ratner, M. A. *J. Chem. Phys.*, in press.

(65) Cohen, M. H.; Lekner, J. *Phys. Rev.* **1967**, *158*, 305. Davis, H. T.; Brown, R. G. *Adv. Chem. Phys.* **1975**, *31*, 329.